A&A 437, 699–702 (2005)
DOI: 10.1051/0004-6361:20042435

Astronomy & Astrophysics

Comments on "Full-sphere simulations of circulation-dominated solar dynamo: Exploring the parity issue"

M. Dikpati, M. Rempel, P. A. Gilman, and K. B. MacGregor

High Altitude Observatory, National Center for Atmospheric Research, PO Box 3000, Boulder, Colorado 80307, USA
e-mail: dikpati@hao.ucar.edu

Received 3 December 2004 / Accepted 22 March 2005

Abstract. Using two distinct simulation codes that respectively apply semi-implicit and fully explicit schemes, we perform calculations of a 2D kinematic Babcock-Leighton type flux-transport dynamo with Chatterjee et al.'s parameter settings. We show that their solutions are diffusion-dominated, rather than circulation-dominated as their title implies. We also have been unable to reproduce several properties of their dynamo solutions, namely we obtain a much faster cycle with ∼4 times shorter period than theirs, with highly overlapping cycles; a polar field value of ∼2 kG if one has to produce a ∼100 kG toroidal field at convection zone base; and quadrupolar parity as opposed to Chatterjee et al.'s dipolar parity solutions.

Key words. Sun: magnetic fields – methods: numerical

1. Introduction

Recently Chatterjee et al. (2004), hereafter CNC, have published a new study of how flux transport dynamos, widely used to model the solar dynamo, select a dominant parity of the solution about the equator. This question is important because by Hale's polarity laws the Sun clearly favor models which select toroidal and poloidal fields that are antisymmetric about the equator. A key difference between their dynamo and others' is that they assume different turbulent diffusivities for toroidal and poloidal fields. Their results show that, by greatly increasing the assumed ohmic diffusivity for poloidal fields in the convection zone, while retaining much lower values for the toroidal field, they eliminate the need for including a tachocline-level α-effect to help select a predominantly antisymmetric field, as was shown to work in Dikpati and Gilman (2001).

Using two quite distinct dynamo simulation codes, that have the same physics included, but completely different numerics, we have been unable to reproduce several properties of their dynamo solutions.

2. Our calculations with two different numerical techniques

We perform numerical simulations with two different codes developed by us. The first is the same as that described in detail in Dikpati & Charbonneau (1999). It uses a semi implicit method, and fits the top boundary to a potential field. The second code, developed more recently by Rempel, is fully explicit, uses a MacCormack differencing scheme, and fits to a radial field boundary condition at the top. We find that the differences in top boundary condition have little effect, and solutions using the two algorithms are generally quite similar.

3. Differences in solutions between our calculations and CNC

3.1. Advection or diffusion dominated solutions

The title of CNC implies that the solutions found are in the part of parameter space where advection by the meridional circulation dominates over diffusion. This claim is made even though all of the interpretations of the solutions are made in terms of diffusion effects. In fact, for their dominant case of high diffusivity for the poloidal field (which is the primary component that is advected to the poles at the top, and then down into the interior and back toward the equator), their solutions are in a diffusion dominated regime. While the solar dynamo is not obliged to be a circulation-dominated dynamo, CNC dynamo appears to be a diffusion-dominated dynamo. For a poloidal diffusivity, η_p, of 2.4×10^{12} cm^2 s^{-1} that they assume within the convection zone, the time it takes for freshly produced poloidal field near the top (in their model the only place it is produced) to diffuse to near the bottom at the same latitude is between 5 and 1.2 years, depending on whether one chooses the total thickness of the shell or half of it. As seen in Fig. 1, where we have plotted streamlines for the meridional circulation CNC chose, and added dots to streamlines signifying the distance traveled in 1 year, the time required to get from mid latitudes at the top to midlatitudes at the bottom is about 20 years. This is the relevant track, since it is the poloidal field at midlatitudes at the bottom that is sheared into toroidal field there to produce the flux that rises to form spots. Even if one computes the time

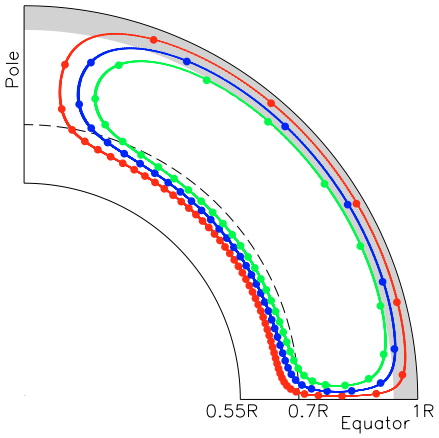

Fig. 1. Dots are plotted in 1-year interval following meridional flow streamlines constructed using CNC parameters. A few selected streamlines that pass through Babcock-Leighton surface source (gray patch) region are presented.

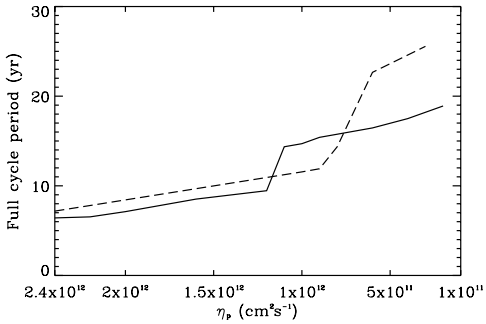

Fig. 2. Cycle period as function of poloidal diffusivity η_p. Solid curve represents a case with a fixed maximum surface flow speed of 32 m s^{-1} as used by CNC; dashed curve represents a case with a fixed surface flow speed of about 21 m s^{-1}. Jump in cycle period below a certain η_p demonstrates transition of a dynamo from diffusion-dominated to advection-dominated regime. The toroidal diffusivity η_t is the same as in CNC's Fig. 4 with $\eta_t = 4 \times 10^{10}$ cm^2 s^{-1}.

from high latitudes at the top to, say, 50° latitude at the bottom, the time elapsed is still >10 years. Hence our conclusion that the CNC dynamo is diffusion dominated, particularly for the diffusivity profiles they display in their Fig. 4, which result in their model selecting dipole symmetry.

The effect of the high diffusion is to "short circuit" the conveyor belt that is the meridional circulation, which should lead to a shorter period for the same meridional circulation. We can see this also in Fig. 2, which plots the dynamo period we have found as a function of the poloidal diffusivity (η_p) of the convection zone, from 2.4×10^{12} cm^2 s^{-1} down to 10^{11} cm^2 s^{-1}, for a toroidal diffusivity η_t the same as in CNC's Fig. 4, $\eta_t = 4 \times 10^{10}$ cm^2 s^{-1} in the convection zone. For the same meridional circulation, the dynamo period remains in the range 7–9 years as η_p is decreased down to about 10^{12} cm^2 s^{-1}, below which it rises steeply to about 13–19 years for $\eta_p \lesssim 10^{12}$ cm^2 s^{-1}, switching to the advection-dominated regime. The value of η_p for this transition largely depends on the selected amplitude of meridional flow. Since CNC uses a maximum surface flow speed of ~32 m s^{-1} that occurs around 70° latitude, the transition from diffusion-dominated regime to the advection-dominated regime takes place at $\eta_p \sim 10^{12}$ cm^2 s^{-1}. For a more solar-like maximum surface flow speed of about 20 m s^{-1} with CNC profiles, the dynamo remains in the diffusion dominated regime for an η_p down to 6×10^{11} cm^2 s^{-1}.

Understanding whether a solution is diffusion or advection dominated is important for interpreting physically what it means. The previous solutions found in Dikpati & Charbonneau (1999); Dikpati & Gilman (2001); Dikpati et al. (2004) are all clearly in the advection dominated regime, while those of CNC are not. In Dikpati & Charbonneau (1999); Dikpati & Gilman (2001); Dikpati et al. (2004) solutions, the dynamo period is approximately inversely proportional to the equatorward meridional flow speed near the bottom. Also, in the diffusion dominated regime, the influence of the upper boundary condition is much stronger than in the advection dominated case, because whatever is applied there diffuses rapidly to the bottom. In the advection dominated case, the influence is less, because the internal advection by the meridional circulation sweeps the internally generated poloidal field away from the upper boundary condition. This property will be very important in interpreting the difference between our results concerning symmetry selection, and that of CNC.

3.2. Dynamo periods

We have performed our simulations by using both the numerical techniques described in Sect. 2, for cases with Babcock-Leighton α-effect, diffusivities and meridional circulation as used by CNC.

The result is that both simulations give full dynamo periods in the neighborhood of 6 to 7 years, in contrast to the 25 year period quoted in CNC, i.e. a factor of ~4 shorter. We find similarly shorter periods with our calculations when we compared to the results of Nandy & Choudhuri (2002) who quoted 15 years there, and we obtained about 3 to 4 years. We have no certain explanation for this difference.

We implement the buoyancy algorithm of CNC by adding the toroidal field from the bottom to the surface layers at the time intervals used by CNC (8.8×10^5 s), but we find no supercritical dynamo solutions; all solutions decay away. This happens because the high magnetic diffusivity near the surface, coupled with the upper boundary condition of zero toroidal field, cause the added toroidal fields to diffuse out of the dynamo domain too quickly. So we have applied the buoyancy mechanism as described in Dikpati & Charbonneau (1999) that includes a non-local Babcock-Leighton α-effect. We explored cases with and without flux-depletion at the bottom, and we obtain similar results in both cases.

We note finally that Nandy & Choudhuri (2001) showed (see Sect. 3.2 therein) that the switching off the depletion of the magnetic field at the base of the convection zone increased the dynamo period. Therefore, it seems unlikely that their buoyancy prescription alone can explain the difference between our dynamo cycle periods and those of CNC.

3.3. Differences in toroidal and poloidal field structures

A further noteworthy difference between our simulations and those of CNC is that while we get time-latitude plots for the toroidal field similar to that shown (with very compressed time scale) in Fig. 7 of CNC, our poloidal fields in both simulations look nothing like the snapshot poloidal fields of their Fig. 8. Typical examples are seen in Fig. 3. Instead, in both cases we get multilobed poloidal fields (typically 3 to 4 in each hemisphere) which to us is more consistent with the multiple overlapping toroidal fields of opposite signs implied (but hard to discern due to the compressed time scale) in their Fig. 7, and seen in our Fig. 4. It is unclear to us how the one extended pole-to-pole dipolar poloidal field CNC show in their Fig. 8b, can create the multilobed toroidal field they show in Fig. 8a within a domain of positive radial shear. In any case, multiple peaks in poloidal and toroidal fields, of alternating sign, present in a hemisphere at the same time, is much different than the Sun, because it means there are several magnetic half cycles visible at the same time. On the other hand, this result is not surprising in view of the extremely high α-effect assumed, which produces extremely strong poloidal fields very quickly.

3.4. TF/PF ratios

Observational estimates of longitude-averaged surface flux from the active region decay (Wang et al. 2000) indicate that about 10% contributes to the transport of flux to the poles to change the sign of polar fields, with the rest cancelled out before it gets to polar regions. This corresponds to a surface α-effect of $\sim$1 m s^{-1} as taken by Dikpati et al. (2004); Wang et al. (2002); Schrijver & De Rosa (2002). The α-effect of 25 m s^{-1} assumed by CNC is therefore sufficiently high that it would require much more than 100% of the Babcock-Leighton poloidal source term estimated from surface observations.

Because of the extremely high α-effect required in CNC to sustain a dynamo, due to the high poloidal diffusivity, polar fields are unusually strong. As produced in our calculations for their parameter values, polar fields are of order 2 kG, when the toroidal field generated is of order 100 kG, which CNC agree is needed to produce spots at low latitudes. But solar observations (Arge et al. 2002) indicate that polar fields are closer to 10 Gauss. As seen in solutions of Dikpati et al. (2002, 2004), solutions that have much more realistic polar fields that also satisfy other major observational characteristics of the solar cycle are available.

3.5. Symmetry selection

Figure 3, obtained by running our simulations with CNC settings of parameters, does not indicate the dynamo relaxing into the dipole mode (antisymmetric magnetic fields about the equator). Instead we find (Fig. 4) that the larger diffusivity makes the dynamo switch much faster to the quadrupole parity than found in a low diffusivity case. If we perform our calculations of the dynamo with CNC settings, it switches to the quadrupolar parity in just 300 to 400 years when initialized by a dipolar mode, in just 15 to 20 years when initialized by random

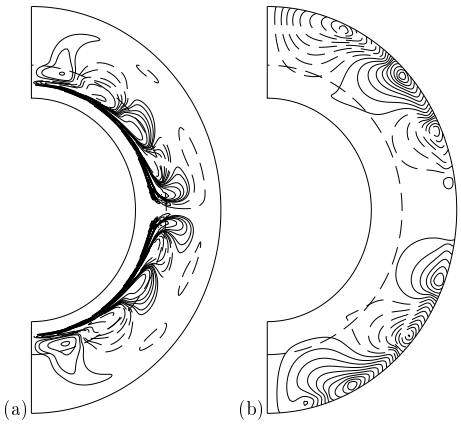

Fig. 3. *Left* and *right* frames respectively show toroidal and poloidal fields at a selected phase of the cycle, obtained in our calculations using CNC parameter settings for their Fig. 7.

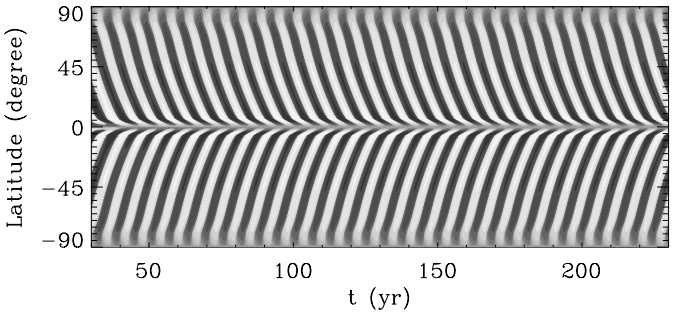

Fig. 4. Butterfly diagram derived from our calculations using CNC parameter settings for their Fig. 8.

numbers, and stays in quadrupole mode for ever when initialized by a quadrupole mode. In fact, all of the solutions we found whose periods are given in Fig. 2 are quadrupolar, in contrast to CNC whose solutions for highest poloidal diffusivity ($\eta_p = 2.4 \times 10^{12}$ cm^2 s^{-1}) are dipolar.

We refer the readers to the Sect. 4.5 of Dikpati & Gilman (2001) for details on the conversion of the Dikpati & Charbonneau (1999) code from hemispheric calculations to full spherical shell calculations that allow us to address the symmetry selection question. As stated in Sect. 3.1 above, the influence of whatever boundary condition is imposed on the poloidal field at the outer boundary is much stronger in diffusion-dominated solutions (left of the period change in Fig. 2) than in the circulation dominated solutions (right of the period change in Fig. 2). To investigate this point, we selected two cases of poloidal diffusivity values, one each from the diffusion-dominated and advection-dominated regimes. We simulated the full-spherical shell dynamo by artificially imposing dipolar conditions at the upper boundary; in this artificial case we found a dipole solution, for example, with an η_p of 2×10^{12} cm^2 s^{-1}, but a quadrupole solution with an η_p of 5×10^{11} cm^2 s^{-1}. Thus the imposition of a particular symmetry at the top is followed by the dynamo in the high diffusion, but not in the low diffusion case.

4. Discussion

CNC have in several places argued that the meridional circulation could get significantly below $r = 0.713R$, where helioseismic measurements say the temperature gradient changes from being essentially adiabatic, to the radiative gradient characteristic of the radiative interior. The results of Gilman and Miesch (2004) preclude that possibility, even to the point of excluding the part of CNC meridional circulation profile (in their Fig. 3), below $r = 0.713R$. In fact, Nandy & Choudhuri (2002) had a subsurface return flow of about a $10\,\mathrm{m\,s^{-1}}$ at $r = 0.6R$. Gilman & Miesch (2004) showed that the penetration below $0.713R$ is limited to at most a few tens of kilometers, no more than 0.0001 of the solar radius, which is no more than 10^{-3} of the distance between $0.7R$ and $0.6R$.

We acknowledge that Dikpati & Charbonneau (1999) used an equatorward return flow which penetrated slightly below $0.7R$, but the purpose of that paper was to demonstrate the properties of a Babcock-Leighton flux-transport dynamo model with solar-like internal rotation pattern and with some interface dynamo features, such as depth-dependent diffusivity, incorporated for the first time into a flux-transport model. Given the knowledge available at that time about the meridional circulation, it was reasonable to try what Dikpati & Charbonneau (1999) did, but not in 2004 when the theory of meridional circulation (Gilman & Miesch 2004) has been developed further. In subsequent papers Dikpati and colleagues did not use such penetration while doing more realistic comparisons between the model output and observed solar cycle features (Dikpati et al. 2004), and got excellent agreement with solar cycle observations. Thus assuming a deep penetration of the meridional flow is not necessary for producing dynamo solutions that agree closely with solar observations.

The concept that there could be separate diffusivities for poliodal and toroidal fields at the same point in the fluid as suggested by CNC appears to be physically implausible. There are not separate conducting fluids for toroidal and poloidal fields, only one fluid that contains them both. Furthermore, the fields themselves are not separate, but linked by continuous field lines. Finally, whatever the turbulence is that causes the diffusion, it is the same for both toroidal and poloidal fields at the same physical point in space. If it is partially suppressed where the toroidal field is strong, the poloidal field feels that suppression too. Despite our doubts concerning the plausibility of separate diffusivities for poloidal and toroidal fields, in all the calculations reported above we have used separate diffusivities to make the comparison with CNC results.

5. Concluding remarks

By utilizing the same parameter regime using two different numerical codes, we have raised a number of questions concerning the results in CNC related to the solar dynamo. We do this to inform the community of solar dynamo modelers, as well as in the hope of resolving the questions we have raised by constructive exchanges in print. Lasting progress in understanding the solar dynamo is best served by agreement on what are valid physical and mathematical descriptions of how this dynamo works.

Acknowledgements. We wish to thank Peter Fox for his constructive criticisms on the earlier version of the manuscript and Giuliana de Toma for a thorough review of the manuscript.

References

Arge, C. N., Hildner, E., Pizzo, V. J., & Harvey, J. W. 2002, J. Geophys. Res., 107, 1319
Bonanno, A., Elstner, D., Rüdiger, G., & Belvedere, G. 2002, A&A, 390, 673
Chatterjee, P., Nandy, D., & Choudhuri, A. R. 2004, A&A, 427, 1019
Dikpati, M., & Charbonneau, P. 1999, ApJ, 518, 508
Dikpati, M., & Gilman, P. A. 2001, ApJ, 559, 428
Dikpati, M., Corbard, T., Thompson, M. J., & Gilman, P. A. 2002, ApJ, 575, L41
Dikpati, M., de Toma, G., Gilman, P. A., Arge, C. N., & White, O. R. 2004, ApJ, 601, 1136
Gilman, P. A., & Miesch, M. S. 2004, ApJ, 611, 568
Nandy, D., & Choudhuri, A. R. 2001, ApJ, 551, 576
Nandy, D., & Choudhuri, A. R. 2002, Science, 296, 1671
Rempel, M., Dikpati, M., & MacGregor, K. B. 2004, Proc. of cool star meeting, in press
Schrijver, C. J., & De Rosa, M. L. 2002, SolP, 212, 165
Wang, Y. -M., Sheeley, N. R., Jr., & Lean, J. L. 2000, Geophys. Res. Lett., 27, 621
Wang, Y. -M., Sheeley, N. R., Jr., & Lean, J. L. 2002, ApJ, 580, 1188